

Novel Zinc Phosphate Topologies Defined by Organic Ligands

Jian Fan and Brian E. Hanson*

Department of Chemistry, Virginia Polytechnic Institute and State University,
Blacksburg, Virginia 24061

Received March 1, 2005

Six new zinc phosphates $[\text{C}_{18}\text{H}_{20}\text{N}_4][\text{Zn}_4(\text{HPO}_4)_4(\text{H}_2\text{PO}_4)_2(\text{C}_{18}\text{H}_{18}\text{N}_4)_3]\cdot 2\text{H}_2\text{O}$ (**1**), $[\text{Zn}_4(\text{HPO}_4)_4(\text{C}_{18}\text{H}_{18}\text{N}_4)_3]\cdot 4\text{H}_2\text{O}$ (**2**), $[\text{Zn}_3(\text{HPO}_4)_3(\text{H}_2\text{PO}_4)(\text{C}_{22}\text{H}_{22}\text{N}_8)_{0.5}(\text{C}_{22}\text{H}_{24}\text{N}_8)_{0.5}]$ (**3**), $[\text{Zn}_2(\text{HPO}_4)_2(\text{C}_{18}\text{H}_{16}\text{N}_4)]$ (**4**), $[\text{Zn}(\text{HPO}_4)(\text{C}_{18}\text{H}_{14}\text{N}_2)]$ (**5**), and $[\text{Zn}_2(\text{HPO}_4)_2(\text{C}_{12}\text{H}_{10}\text{N}_4)]$ (**6**) have been synthesized under mild hydrothermal conditions in the presence of 1,4-bis(*N*-benzimidazolyl)butane (L1), 1,2,4,5-tetrakis(imidazol-1-ylmethyl)benzene (L2), 1,4-bis(imidazol-1-ylmethyl)naphthalene (L3), 9-(imidazol-1-ylmethyl)anthracene (L4), and 1,4-bis(1-imidazolyl)benzene (L5), respectively, and their structures were determined by X-ray crystallography. Compound **1** exhibits a unique inorganic motif of isolated 8-rings interconnected by L1. Compound **2**, also formed from L1, contains a previously unobserved chain structure composed of edge-sharing 4-rings and 8-rings. Compound **3**, prepared from L2, possesses an unusual one-dimensional framework, which is composed of vertex-sharing 4-rings and triple fused 4-rings. The inorganic portions of **4**, **5**, and **6** each adopt a layer structure. The sheets in **4** and **5** have a 4.8^2 topology, and in **6**, a 6^3 topology is observed. The zinc atoms in compounds **1**–**6** are all tetrahedrally coordinated by a combination of phosphate groups and organic ligands. Potential relationships between the inorganic motifs reported in the present study are identified. These are indicative of a possible pattern of self-assembly of zinc and phosphorus tetrahedra and indicative of the role of the organic ligands in the formation of hybrid structures.

Introduction

Framework zinc materials including zinc phosphates are of considerable interest due to their wide application in the areas of separation, catalysis, and absorption.¹ The synthesis of zinc phosphates with zero-, one-, two-, and three-dimensional (3D) structures has been successfully achieved during the past decade.^{2,3} Two commonly observed features

of the observed structures are that the inorganic frameworks are often anionic and a protonated organic amine, used as a templating agent, directs the structure formation by filling the void space and interacting with the framework with multipoint $\text{N}-\text{H}\cdots\text{O}_f$ (f = framework) hydrogen bonds.⁴ For example, Rao and co-workers developed a simple universal route in which the reaction of amine phosphate and metal ions yields a hierarchy of templated structures.^{2b} Further, it is observed that phosphorus groups modified by organic units are very effective in the construction of hybrid materials.⁵ Until recently, hybrid zinc phosphates/phosphites that contain direct Zn–N bonds have been rarely reported.⁶ In these cases, the organic groups coordinate to the metal ions of the framework and act as structure-building units. Harrison, for example, reported α - and β - $\text{ZnHPO}_3\cdot\text{N}_4\text{C}_2\text{H}_4$ as the first organically modified zinc phosphites.^{6a} The ligands 2,2'-dipyridine⁷ and imidazoles^{6c,8} have also been reported to

* To whom correspondence should be addressed. E-mail: hanson@vt.edu.

- (1) (a) Rao, C. N. R.; Natarajan, S.; Choudhury, A.; Neeraj, S.; Ayi, A. *Acc. Chem. Res.* **2001**, *34*, 80. (b) Murugavel, R.; Walawalkar, D. M.; Roesky, H. W.; Rao, C. N. R. *Acc. Chem. Res.* **2004**, *37*, 409. (c) Cheetham, A. K.; Férey, G.; Loiseau, T. *Angew. Chem., Int. Ed.* **1999**, *38*, 3268. (d) Pan, J. X.; Zheng, S. T.; Yang, G. Y. *Cryst. Growth Des.* **2005**, *5*, 231. (e) Wang, Y.; Yu, J.; Guo, M.; Xu, R. *Angew. Chem., Int. Ed.* **2003**, *42*, 4089.
- (2) (a) Jensen, T. R.; Gerentes, N.; Jepsen, J.; Hazell, R. G.; Jakobsen, H. *J. Inorg. Chem.* **2005**, *44*, 658. (b) Rao, C. N. R.; Natarajan, S.; Neeraj, S. *J. Am. Chem. Soc.* **2000**, *122*, 2810. (c) Neeraj, S.; Natarajan, S.; Rao, C. N. R. *J. Solid State Chem.* **2000**, *150*, 417. (d) Harrison, W. T. A.; Hanooman, L. *J. Solid State Chem.* **1997**, *131*, 363. (e) Yang, G.-Y.; Sevov, S. C. *J. Am. Chem. Soc.* **1999**, *121*, 8389. (f) Norquist, A. J.; O'Hare, D. *J. Am. Chem. Soc.* **2004**, *126*, 6673.
- (3) (a) Liu, W.; Liu, Y.; Shi, Z.; Pang, W. *J. Mater. Chem.* **2000**, *10*, 1451. (b) Song, Y.; Yu, J.; Li, Y.; Zhang, M.; Xu, R. *Eur. J. Inorg. Chem.* **2004**, 3718. (c) Choudhury, A.; Neeraj, S.; Natarajan, S.; Rao, C. N. R. *J. Mater. Chem.* **2001**, *11*, 1537. (d) Natarajan, S.; Wullen, L. V.; Klein, W.; Jansen, M. *Inorg. Chem.* **2003**, *42*, 6265.

- (4) Gordon, L. E.; Harrison, W. T. A. *Inorg. Chem.* **2004**, *43*, 1808.
- (5) Shi, X.; Zhu, G.; Qiu, S.; Huang, K.; Yu, J.; Xu, R. *Angew. Chem., Int. Ed.* **2004**, *43*, 6482. (b) Cao, D. K.; Gao, S.; Zheng, L. M. *J. Solid State Chem.* **2004**, *177*, 2311. (c) Gómez-Alcántara, M. M.; Cabeza, A.; Martínez-Lara, M.; Aranda, M. A. G.; Suau, R.; Bhuvanesh, N.; Clearfield, A. *Inorg. Chem.* **2004**, *43*, 5283. (d) Lei, C.; Mao, J. G.; Sun, Y. Q. *J. Solid State Chem.* **2004**, *177*, 2449; (e) Clearfield, A. *Prog. Inorg. Chem.* **1998**, *47*, 375 and references therein.

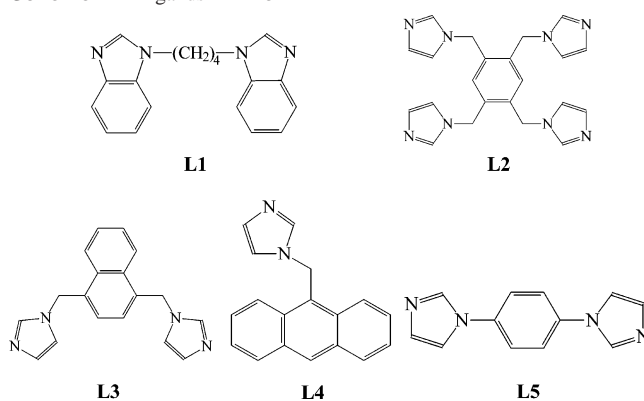
Table 1. Crystal Data and Structure Refinement Parameters for 1–6

structure parameter	1	2	3	4	5	6
empirical formula	C ₃₆ H ₄₃ N ₈ O ₁₃ P ₃ Zn ₂	C ₂₇ H ₃₃ N ₆ O ₁₀ P ₂ Zn ₂	C ₂₂ H ₂₈ N ₈ O ₁₆ P ₄ Zn ₃	C ₉ H ₉ N ₂ O ₄ PZn	C ₁₈ H ₁₅ N ₂ O ₄ PZn	C ₆ H ₆ N ₂ O ₄ PZn
fw	1019.43	794.27	980.51	305.52	419.66	266.47
T (K)	100	100	100	100	100	100
space group	P $\bar{1}$	P $\bar{1}$	P2 ₁ /c	Pnma	P2 ₁ /c	P2 ₁ /n
a (Å)	10.3187(10)	9.0382(9)	14.9410(10)	8.7620(7)	19.715(3)	5.2956(6)
b (Å)	13.6651(14)	13.6616(10)	14.6445(7)	28.368(3)	8.4865(10)	20.243(2)
c (Å)	16.1419(16)	13.7094(9)	15.8209(11)	8.7638(7)	9.9938(10)	7.5816(9)
α (deg)	102.047(8)	99.997(6)				
β (deg)	108.580(9)	101.158(7)	109.503(6)		95.485(9)	100.041(10)
γ (deg)	99.147(8)	108.140(8)				
V (Å ³)	2046.6(4)	1527.8(2)	3263.1(4)	2178.3(3)	1664.4(3)	800.29(16)
Z	2	2	4	8	4	4
D _{calc} (g cm ⁻³)	1.654	1.727	1.996	1.863	1.675	2.212
μ (mm ⁻¹)	1.365	1.743	2.472	2.405	1.600	3.255
R ₁ ^a [I > 2 σ (I)]	0.0613	0.0475	0.0388	0.0608	0.0689	0.0370
wR ₂ ^b [I > 2 σ (I)]	0.1452	0.1263	0.1030	0.1117	0.1536	0.0863

^a $R_1 = \sum |F_o| - |F_c| / \sum |F_o|$. ^b $wR_2 = \{[\sum (w(F_o^2 - F_c^2))^2] / [\sum (w(F_o^2))^2]\}^{1/2}$, where $w = 1/[\sigma^2(F_o) + (aP)^2 + bP]$ and $P = [(F_o)^2 + 2(F_c)^2]/3$.

decorate metal ions in the synthesis of hybrid networks. Recently, we have shown that bisimidazole ligands are very effective in organizing zinc phosphates and zinc phosphites into new structures.^{9,10} For example, 1,4-bis(imidazol-1-ylmethyl)benzene knits the well-known zinc phosphate ladder structure together to form a hybrid sheet,⁹ and 1,3-bis(imidazol-1-ylmethyl)benzene ties zinc phosphite stair steps into a 3D network.¹⁰

Despite the discovery of numerous compounds with novel structures, the understanding of the formation of zinc phosphates/phosphites continues to be poor.^{3d} Here, we use a series of multifunctional organic ligands to modify the aggregation of the zinc and phosphorus tetrahedra, to obtain information on how the tailored inorganic pieces can be connected. Six new zinc phosphates are reported, [C₁₈H₂₀N₄]-[Zn₄(HPO₄)₄(H₂PO₄)₂(C₁₈H₁₈N₄)₃] \cdot 2H₂O (**1**), [Zn₄(HPO₄)₄(C₁₈H₁₈N₄)₃] \cdot 4H₂O (**2**), [Zn₃(HPO₄)₃(H₂PO₄)₃(C₂₂H₂₂N₈)_{0.5}]-[C₂₂H₂₄N₈]_{0.5} (**3**), [Zn₂(HPO₄)₂(C₁₈H₁₆N₄)] (**4**), [Zn(HPO₄)(C₁₈H₁₄N₂)] (**5**), and [Zn₂(HPO₄)₂(C₁₂H₁₀N₄)] (**6**). The zinc atoms are decorated by the ligands shown in Scheme 1: 1,4-bis(*N*-benzimidazolyl)butane (L1), 1,2,4,5-tetrakis(imidazol-1-ylmethyl)benzene (L2), 1,4-bis(imidazol-1-ylmethyl)naphthalene (L3), 9-(imidazol-1-ylmethyl)anthracene (L4), and 1,4-bis(1-imidazolyl)benzene (L5).

Scheme 1. Ligands L1–L5

Experimental Section

Materials and Measurements. All commercially available chemicals are of reagent grade and used as received without further purification. The ligands 1,4-bis(*N*-benzimidazolyl)butane (L1),¹¹ 1,2,4,5-tetrakis(imidazol-1-ylmethyl)benzene (L2),¹² 1,4-bis(imidazol-1-ylmethyl)naphthalene (L3),¹³ 9-(imidazol-1-ylmethyl)anthracene (L4),¹⁴ and 1,4-bis(1-imidazolyl)benzene (L5)¹⁵ were synthesized according to the literature. Elemental analyses of C, H, and N were performed by Galbraith Laboratories, Inc. Emission spectra were recorded on a PTI Alphascan fluorimeter with a thermoelectrically cooled R666S photomultiplier tube.

All the syntheses of hybrid materials in this paper were carried out in heavy-wall tubes with a fill factor of 40%. **Caution:** The tubes are potentially explosive under high temperature and pressure and should be handled with care. The pH values were measured with pH paper before and after reaction. The pH of the systems is in the range of 5–7 and does not appear to change significantly during the course of the reaction.

[C₁₈H₂₀N₄][Zn₄(HPO₄)₄(H₂PO₄)₂(C₁₈H₁₈N₄)₃] \cdot 2H₂O (**1**) and [Zn₄(HPO₄)₄(C₁₈H₁₈N₄)₃] \cdot 4H₂O (**2**). Hydrothermal treatment of zinc acetate dehydrate (219.5 mg, 1.0 mmol), phosphoric acid (85

- (6) (a) Harrison, W. T. A.; Phillips, M. L. F.; Stanchfield, J.; Nenoff, T. M. *Inorg. Chem.* **2001**, *40*, 895. (b) Kirkpatrick, A.; Harrison, W. T. A. *Solid State Sci.* **2004**, *6*, 593. (c) Cui, A.; Yao, Y. *Chem. Lett.* **2001**, 1148. (d) Neeraj, S.; Natarajan, S.; Rao, C. N. R. *New J. Chem.* **1999**, 303. (e) Rodgers, J. A.; Harrison, W. T. A. *Chem. Commun.* **2000**, 2385. (f) Ayi, A. A.; Choudhury, A.; Natarajan, S.; Rao, C. N. R. *J. Mater. Chem.* **2001**, *11*, 1181. (g) Choudhury, A.; Natarajan, S.; Rao, C. N. R. *Inorg. Chem.* **2000**, *39*, 4295. (h) Liang, J.; Wang, Y.; Yu, J.; Li, Y.; Xu, R. *Chem. Commun.* **2003**, 882.
- (7) (a) Hagrman, P. J.; Hagrman, D.; Zubieta, J. *Angew. Chem., Int. Ed.* **1999**, *38*, 2638. (b) Lin, Z.; Zhang, J.; Yang, G. *Inorg. Chem.* **2004**, *43*, 797. (c) Lin, Z.; Zhang, J.; Zheng, S.; Yang, G. *Inorg. Chem. Commun.* **2003**, *6*, 1035. (d) Mandal, S.; Pati, S. K.; Green, M. A.; Natarajan, S. *Chem. Mater.* **2005**, *17*, 638.
- (8) (a) Xing, Y.; Liu, Y.; Shi, Z.; Zhang, P.; Fu, Y.; Cheng, C.; Pang, W. *J. Solid State Chem.* **2002**, *163*, 364. (b) Natarajan, S.; Neeraj, S.; Rao, C. N. R. *Solid State Sci.* **2000**, *2*, 87.
- (9) Fan, J.; Slebodnick, C.; Angel, R.; Hanson, B. E. *Inorg. Chem.* **2005**, *44*, 552.
- (10) Fan, J.; Slebodnick, C.; Troya, D.; Angel, R.; Hanson, B. E. *Inorg. Chem.* **2005**, *44*, 2719.

- (11) Shi, Z. Q.; Thummel, R. P. *J. Org. Chem.* **1995**, *60*, 5935.
- (12) Murai, S.; Mikoshiba, S.; Sumino, H.; Hayase, S. *J. Photochem. Photobiol., A* **2002**, *148*, 33.
- (13) Zou, R.; Xu, F.; Li, Q.; Zhang, Z. *Acta Crystallogr.* **2003**, *E59*, o1451.
- (14) Liu, Q.; Xu, F.; Li, Q.; Zeng, X.; Leng, X.; Chou, Y.; Zhang, Z. *Organometallics* **2003**, *22*, 309.
- (15) Cristau, H.; Cellier, P. P.; Spindler, J.; Taillefer, M. *Chem.—Eur. J.* **2004**, *10*, 5607.

wt %, 230.6 mg, 2.0 mmol), 1,4-bis(*N*-benzimidazolyl)butane (435.0 mg, 1.5 mmol), and water (6 mL) for 10 days at 130 °C yields colorless microcrystalline products **1** and **2**.

[Zn₃(HPO₄)₃(H₂PO₄)(C₂₂H₂₂N₈)_{0.5}(C₂₂H₂₄N₈)_{0.5}] (**3**). Hydrothermal treatment of zinc acetate dihydrate (219.5 mg, 1.0 mmol), phosphoric acid (85 wt %, 230.6 mg, 2.0 mmol), 1,2,4,5-tetrakis-(imidazol-1-ylmethyl)benzene (169.0 mg, 0.5 mmol), and water (6 mL) for 10 days at 130 °C yields several crystalline products, compound **3**, and one additional compound, **7**, that gives crystals of poor quality.¹⁶

[Zn₂(HPO₄)₂(C₁₈H₁₆N₄)] (**4**). Hydrothermal treatment of zinc acetate dihydrate (65.8 mg, 0.3 mmol), potassium dihydrogenphosphate (81.6 mg, 0.6 mmol), 1,4-bis(imidazol-1-ylmethyl)naphthalene (86.4 mg, 0.3 mmol), and water (6 mL) for 10 days at 130 °C yields a plate crystalline product. Yield: 84% on the basis of zinc source. Fourier transform infrared (FT-IR) spectroscopy (cm⁻¹): 3091(w), 1526(m), 1453(m), 1389(m), 1281(w), 1253(w), 1203(m), 1118(m), 1092(s), 1045(m), 1023(s), 974(m), 915(s), 847(m), 807(m), 773(m), 741(s). Thermogravimetric analysis (TGA): <0.2% weight loss to 150 °C. Anal. Calcd for C₉H₉N₂O₄-PZn: C, 35.38; H, 2.97; N, 9.17. Found: C, 35.31; H, 3.19; N, 9.15.

[Zn(HPO₄)(C₁₈H₁₄N₂)] (**5**). Hydrothermal treatment of zinc acetate dihydrate (219.5 mg, 1.0 mmol), phosphoric acid (85 wt %, 115.3 mg, 1.0 mmol), 9-(imidazol-1-ylmethyl)anthracene (258.0 mg, 1.0 mmol), and water (6 mL) for 10 days at 130 °C yields a plate crystalline product. Yield: 65% on the basis of zinc source. FT-IR (cm⁻¹): 3100(w), 1623(w), 1576(w), 1525(m), 1447(m), 1402(m), 1335(m), 1256(m), 1205(m), 1181(m), 1118(m), 1096(m), 1046(s), 1015(s), 949(m), 903(s), 851(m), 799(m), 745(m), 722(s). Fluorescence spectrum (nm, excitation at 350 nm): 421, 446 in a ratio of 1.2/1, 475 (shoulder). TGA: <0.4% weight loss to 150 °C. Anal. Calcd for C₁₈H₁₅N₂O₄PZn: C, 51.52; H, 3.60; N, 6.68. Found: C, 51.25; H, 3.93; N, 6.65.

[Zn₂(HPO₄)₂(C₁₂H₁₀N₄)] (**6**). Hydrothermal treatment of zinc acetate dihydrate (219.5 mg, 1.0 mmol), phosphoric acid (85 wt %, 230.6 mg, 2.0 mmol), 1,4-bis(1-imidazolyl)benzene (315.0 mg, 1.5 mmol), and water (6 mL) for 10 days at 130 °C yields a needle crystalline product. Yield: 77% on the basis of zinc source. FT-IR (cm⁻¹): 3137(w), 1646(m), 1541(m), 1533(m), 1317(m), 1204(m), 1165(m), 1130(m), 1110(m), 1025(s), 960(m), 948(m), 911(s), 846(m), 835(m), 799(m), 770(m). TGA: 140 °C dec. Anal. Calcd for C₆H₆N₂O₄PZn: C, 27.04; H, 2.27; N, 10.51. Found: C, 27.04; H, 2.64; N, 10.41.

Crystallographic Analyses. Low temperature (100 K) single-crystal X-ray diffraction measurements for complexes **1–6** were collected on an Oxford Diffraction Xcalibur2 diffractometer equipped with the Enhance X-ray source and a Sapphire 2 CCD detector. The data collection routine, unit cell refinement, and data processing were carried out with the program CrysAlis.¹⁷ The structure was solved by direct methods using SHELXS-97 and refined by full-matrix least-squares analysis.¹⁸ The final refinements involved an anisotropic model for all non-hydrogen atoms. Hydrogen atoms were either located from the residual e⁻ density map and refined independently or located by a riding model. The hydrogen atoms bonded to the oxygen atom of lattice water

Table 2. Selected Bond Distances (Å) and Angles (deg) for **1–6**^a

1			
Zn1–O2	1.921(3)	Zn1–O12	1.937(3)
Zn1–N1	2.006(4)	Zn1–N5	2.010(4)
Zn2–O8	1.912(3)	Zn2–O4	1.947(3)
Zn2–O11 ^{#1}	1.962(3)	Zn2–N3	2.010(4)
O2–Zn1–O12	120.34(14)	O2–Zn1–N1	107.07(15)
O12–Zn1–N1	112.37(15)	O2–Zn1–N5	102.38(14)
O12–Zn1–N5	107.02(14)	N1–Zn1–N5	106.41(16)
O8–Zn2–O4	109.96(14)	O8–Zn2–O11 ^{#1}	103.34(14)
O4–Zn2–O11 ^{#1}	118.43(13)	O8–Zn2–N3	110.43(15)
O4–Zn2–N3	98.67(15)	O11 ^{#1} –Zn2–N3	116.09(14)
2			
Zn1–O2	1.933(2)	Zn1–O8	1.955(2)
Zn1–N3	1.992(3)	Zn1–N1	2.007(3)
Zn2–O4 ^{#2}	1.911(2)	Zn2–O5 ^{#3}	1.928(2)
Zn2–O3	1.928(2)	Zn2–N5	2.029(3)
O2–Zn1–O8	108.79(9)	O2–Zn1–N3	123.31(10)
O8–Zn1–N3	98.68(10)	O2–Zn1–N1	103.72(10)
O8–Zn1–N1	110.86(10)	N3–Zn1–N1	111.32(11)
O4 ^{#2} –Zn2–O5 ^{#3}	122.54(10)	O4 ^{#2} –Zn2–O3	116.66(10)
O5 ^{#3} –Zn2–O3	104.02(10)	O4 ^{#2} –Zn2–N5	102.52(10)
O5 ^{#3} –Zn2–N5	104.46(10)	O3–Zn2–N5	104.64(10)
3			
Zn1–O3	1.916(3)	Zn1–O11	1.954(3)
Zn1–O7	1.968(3)	Zn1–N3 ^{#4}	2.011(4)
Zn2–O8	1.891(4)	Zn2–O4	1.945(3)
Zn2–O6	1.968(3)	Zn2–N1	1.991(4)
Zn3–O12	1.934(3)	Zn3–O9	1.938(3)
Zn3–O14	1.951(3)	Zn3–N5	2.005(4)
O3–Zn1–O11	110.71(13)	O3–Zn1–O7	114.16(13)
O11–Zn1–O7	103.35(13)	O3–Zn1–N3 ^{#4}	117.10(14)
O11–Zn1–N3 ^{#4}	97.17(14)	O7–Zn1–N3 ^{#4}	112.08(14)
O8–Zn2–O4	105.66(16)	O8–Zn2–O6	124.69(15)
O4–Zn2–O6	99.25(13)	O8–Zn2–N1	106.–05(16)
O4–Zn2–N1	108.64(15)	O6–Zn2–N1	111.40(14)
O12–Zn3–O9	112.40(14)	O12–Zn3–O14	111.80(13)
O9–Zn3–O14	110.89(13)	O12–Zn3–N5	97.78(15)
O9–Zn3–N5	108.72(14)	O14–Zn3–N5	114.66(15)
4			
Zn1–O4	1.920(3)	Zn1–O2	1.938(3)
Zn1–O3	1.956(3)	Zn1–N1	1.998(4)
O4–Zn1–O2	107.13(14)	O4–Zn1–O3	120.76(14)
O2–Zn1–O3	110.31(14)	O4–Zn1–N1	107.31(16)
O2–Zn1–N1	111.67(15)	O3–Zn1–N1	99.41(16)
5			
Zn1–O1	1.919(3)	Zn1–O2	1.957(4)
Zn1–O3	1.964(3)	Zn1–N1	2.008(5)
O1–Zn1–O2	108.26(15)	O1–Zn1–O3	109.81(15)
O2–Zn1–O3	102.94(15)	O1–Zn1–N1	118.12(17)
O2–Zn1–N1	108.15(17)	O3–Zn1–N1	108.49(17)
6			
Zn1–O3	1.9283(14)	Zn1–O1	1.946(3)
Zn1–O4	1.9530(14)	Zn1–N1	2.0028(14)
O3–Zn1–O1	111.04(10)	O3–Zn1–O4	108.16(7)
O1–Zn1–O4	116.61(10)	O3–Zn1–N1	108.27(7)
O1–Zn1–N1	109.06(10)	O4–Zn1–N1	103.19(7)

^a Symmetry transformations used to generate equivalent atoms: (#1) $-x + 1, -y, -z + 2$; (#2) $-x, -y + 2, -z$; (#3) $-x + 1, -y + 2, -z$; (#4) $x, y, z + 1$.

molecules in **1** and **2** were not located. The disordered carbon atoms, C30 (sof: 0.72 and 0.28) in **1** and C27 (sof: 0.63 and 0.37) in **2**, are located with the site occupancy factor (sof) given in the parentheses. The crystal parameters, data collection, and refinement results for compounds **1–6** are summarized in Table 1. Selected bond lengths and angles are listed in Table 2. Further details are provided in the Supporting Information.

Results

Crystal Structures [C₁₈H₂₀N₄][Zn₄(HPO₄)₄(H₂PO₄)₂-(C₁₈H₁₈N₄)₃]·2H₂O (**1**) and [Zn₄(HPO₄)₄(C₁₈H₁₈N₄)₃]·4H₂O

(16) Crystal data for **7**: triclinic, space group $P\bar{1}$, $a = 10.0683$ Å, $b = 14.9733$ Å, $c = 15.6267$ Å, $\alpha = 88.702^\circ$, $\beta = 83.786^\circ$, $\gamma = 89.130^\circ$, $V = 2341.18$ Å³, and $Z = 2$.

(17) CrysAlis, version 1.171; Oxford Diffraction: Wrocław, Poland, 2004.

(18) (a) Sheldrick, G. M. *SHELXS97: Program for Crystal Structure Determination*; University of Göttingen: Germany, 1997. (b) Sheldrick, G. M. *SHELXL97: Program for Crystal Structural Refinement*; University of Göttingen: Germany, 1997.

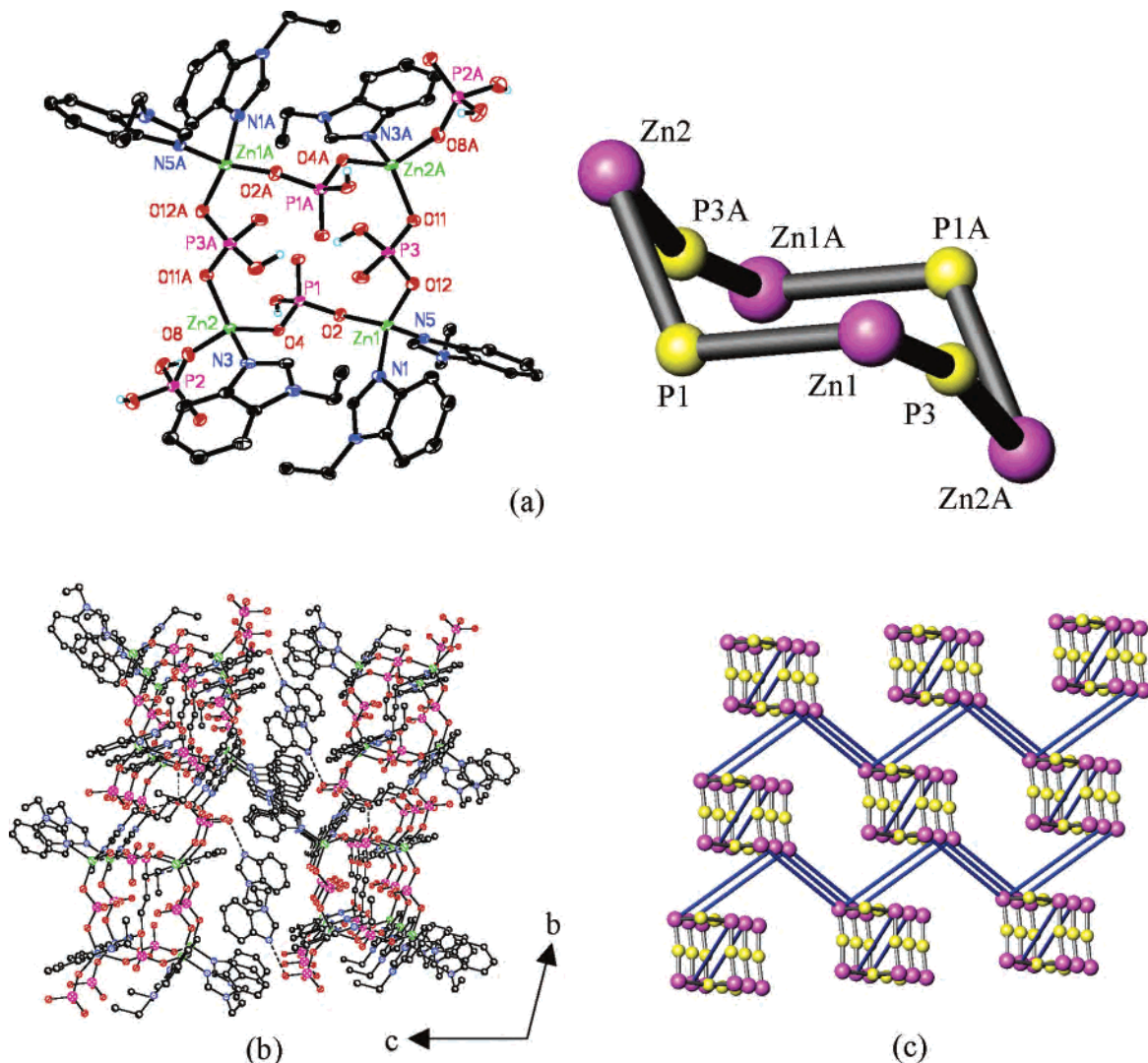


Figure 1. (a) Fragment of the structure of compound **1** showing the atom labeling scheme. Thermal ellipsoids are drawn at 50% probability (left) and the conformation of the 8-ring (right; Zn: pink, P: yellow). (b) Packing diagram of compound **1** with the hydrogen bonds indicated by dashed lines. (c) Schematic drawing of the 3D network in **1** (Zn: pink ball, P: yellow ball).

(2). The reaction of the flexible ligand L1 with zinc phosphate under hydrothermal conditions yields two crystalline phases. Compounds **1** and **2** may be manually separated from the reaction mixture by recognition of their different crystal morphologies.

The asymmetric unit of compound **1** contains two crystallographically distinct zinc atoms and three P atoms. One zinc atom (ZnO_2N_2) is coordinated by two oxygen atoms from phosphate groups with an average Zn–O–P bonding angle of 128.4° and two nitrogen atoms from the L1 units [$(\text{Zn–O})_{\text{av}} = 1.929 \text{ \AA}$ and $(\text{Zn–N})_{\text{av}} = 2.008 \text{ \AA}$]; the other zinc atom (ZnO_3N) is coordinated by three oxygens from phosphate groups with an average Zn–O–P bonding angle of 135.9° and one nitrogen from L1 [$(\text{Zn–O})_{\text{av}} = 1.940 \text{ \AA}$ and $(\text{Zn–N}) = 2.010 \text{ \AA}$]. Of the three phosphorus atoms, P1 and P3 make two P–O–Zn linkages and possess two P–O terminals, an –OH group and an unsaturated =O atom (HPO_4^{2-}), and P2 has one P–O–Zn linkage and three P–O terminals. Thus, P2 is pendant to the zinc phosphate frame. The hydrogen atoms bonded to the phosphorus groups were located in the residual e^- density map and refined indepen-

dently. The three phosphorus atoms have P–O distances in the range of $1.501(4)$ – $1.576(3) \text{ \AA}$ [$(\text{P1–O})_{\text{av}} = 1.533 \text{ \AA}$, $(\text{P2–O})_{\text{av}} = 1.534 \text{ \AA}$, $(\text{P3–O})_{\text{av}} = 1.537 \text{ \AA}$].

An ORTEP diagram of **1** is shown in Figure 1a. The connectivity of zinc (ZnO_2N_2 and ZnO_3N) and phosphorus (HPO_4^{2-}) tetrahedra gives rise to isolated 8-rings with two pendant H_2PO_4^- tetrahedra bonded to zinc atoms at diagonal positions. To the best of our knowledge, compound **1** represents the largest isolated ring in the ZnPO class of compounds. Within each 8-ring, Zn1, Zn1A, P1, and P1A are coplanar. The atoms Zn2 and Zn2A are displaced above and below the plane by 2.5407 \AA , and the atoms P3 and P3A lie 0.9649 \AA above and below the plane. Additionally, the four zinc atoms are coplanar and the four phosphorus atoms are coplanar. Within the 8-ring, the Zn1–P3–Zn2A angle is 166.9° . Thus, the 8-ring adopts a chair conformation, also shown in Figure 1a. The 8-rings are slightly skewed, as seen from the P–P and Zn–Zn distances: P1–P1A = 6.789 \AA ; P2–P2A = 5.234 \AA ; Zn1–Zn1A = 8.559 \AA ; Zn2–Zn2A = 7.651 \AA . The 8-ring is stabilized by hydrogen

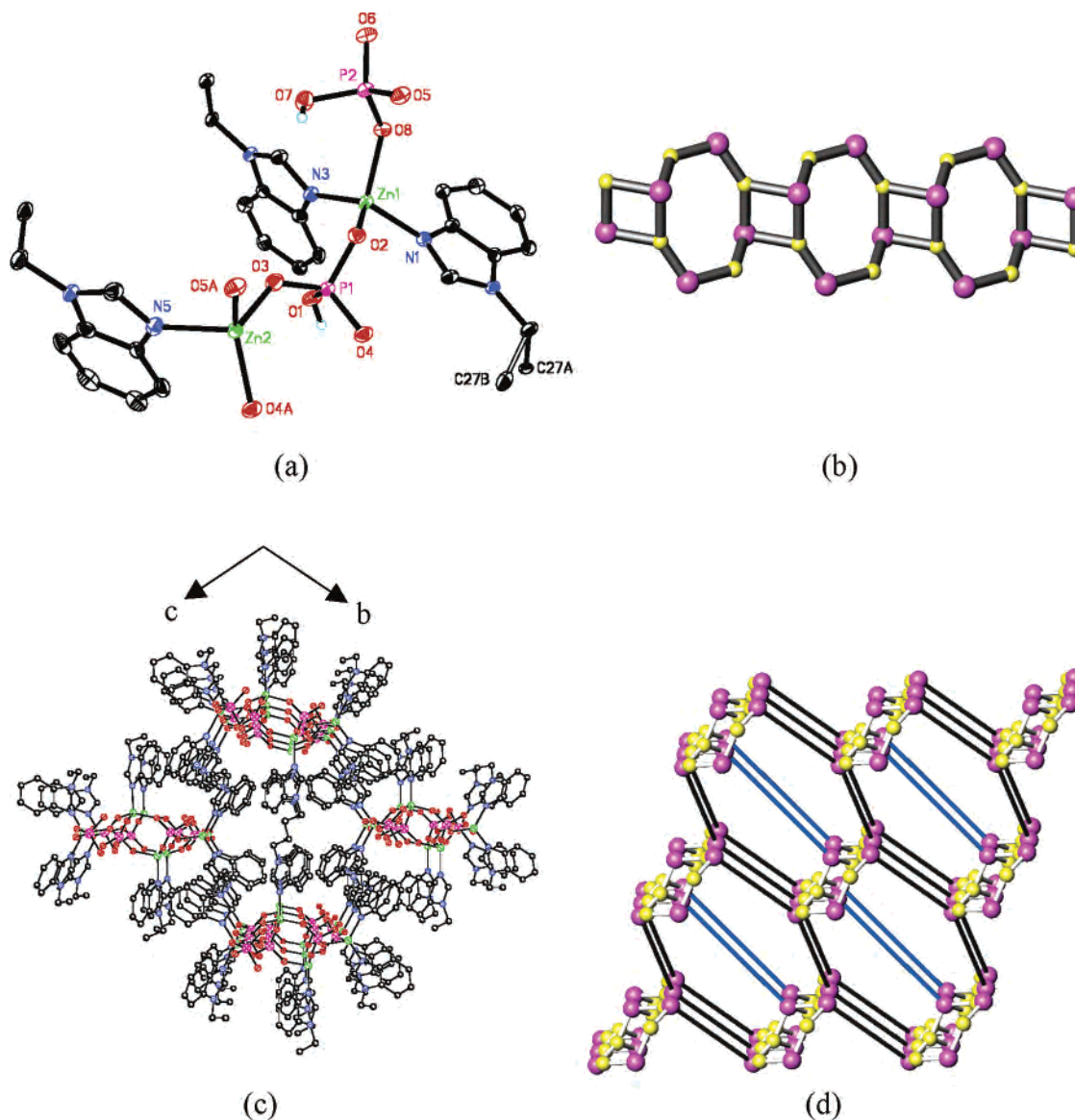


Figure 2. (a) Asymmetric unit of the structure of compound **2** showing the atom labeling scheme. Thermal ellipsoids are drawn at 50% probability. (b) Schematic drawing of the 4.8-chain in **2**. (c) Packing diagram and (d) schematic drawing of compound **2** (Zn: pink ball, P: yellow ball). The connection between ZnO_2N_2 vertexes is indicated by black lines, and the connection between ZnO_3N vertexes, by blue lines.

bonding between intraring phosphate groups; the O10A–O3A distance is 2.571 Å, and the O10A–H3A–O3A angle is 174.9°.

A packing diagram of **1** is shown in Figure 1b. Each 8-ring is connected into a 3D hybrid framework by three ligands; a fourth protonated ligand acts as a template and fills the interstitial space of the framework. A schematic version of the packing diagram is given in Figure 1c, in which the 8-rings are shown with direct connections between zinc and phosphorus and the framework ligands are shown as lines. If each phosphorus atom and zinc atom is considered as a node, then a zigzag hybrid sheet structure that contains alternating 8- and 12-rings of T atoms can be described. The T atoms, however, are not equivalent, each phosphorus atom in the sheet is biconnected, Zn1 is tetraconnected in the sheet, and Zn2 is biconnected in the sheet (with one additional connection to a sheet above or below). The sheets are stacked in an AAA fashion.

The 8-ring stoichiometry of $[\text{Zn}_4(\text{HPO}_4)_4(\text{H}_2\text{PO}_4)_2]^{2-}$ has a net negative charge that is balanced by the protonation of the extraframework ligand.²⁰ The extraframework ligand L1 is located in the pseudo 12-ring channel and acts as a structure-directing agent, through N–H···O hydrogen bond interactions with the H_2PO_4^- groups [(N7···O6) = 2.675(6) Å, and (N7–H7B–O6) = 160°]. Thus, L1 plays an unusual dual role in **1**, as both ligand and template, to stabilize the 3D structure. Such a dual role has rarely been reported.^{6g}

The asymmetric unit of compound **2** contains two crystallographically distinct zinc atoms and two phosphorus atoms, as shown in Figure 2a. One zinc atom is tetrahedrally coordinated by two oxygen atoms from phosphate groups [$(\text{Zn–O–P})_{\text{av}} = 123.6^\circ$] and two nitrogen atoms from the

(19) Harrison, W. T. A.; Nenoff, T. M.; Gier, T. E.; Stucky, G. D. *J. Solid State Chem.* **1994**, *113*, 168.

(20) Due to the low e^- density in channels of this structure, the hydrogen atom attached to the nitrogen atom is added geometrically.

L1 ligands [(Zn–O)_{av} = 1.944 Å and (Zn–N)_{av} = 1.999 Å]; the other zinc is coordinated by three oxygens from phosphate groups [(Zn–O–P)_{av} = 135.4°] and one nitrogen from L1 [(Zn–O)_{av} = 1.922 Å and (Zn–N) = 2.029 Å]. The two phosphorus atoms are connected such that P1 is linked to Zn by three P–O–Zn linkages and P2 is connected to zinc by two P–O–Zn linkages. The longest P–O bond length for the two phosphorus groups is 1.570(2) Å and 1.589(2) Å, respectively, corresponding to the –OH group.²¹ Thus, each phosphorus group is a HPO₄^{2–} anion. To confirm the assignment, the hydrogen atoms attached to the phosphorus group are located in the residual e[–] density map and refined independently. The resulting stoichiometry, Zn₂–(HPO₄)₂, gives a neutral framework.

The inorganic motif in **2** consists of a one-dimensional (1D) polymeric zinc–oxygen–phosphate chain constructed from edge-sharing 4-rings and 8-rings, as illustrated in Figure 2b. The strictly alternating 4-ring and 8-ring pattern appears frequently in zinc phosphates/phosphites, especially in 4.8²-sheets.²² However, isolated 4.8-chains have not been previously reported. The 4.8-chains can form either by joining 8-rings in such a way to create the 4-ring or by forming a simple ladder and cleaving two out of every four rungs in the ladder.

The two zinc atoms with a ZnO₃N coordination set are contained within the 8-rings and 4-rings; the two zinc atoms that have a ZnO₂N₂ coordination set are only found in the 8-rings. In **2**, the chain structures are parallel and propagate along the [100] direction, as shown in Figure 2c. In Figure 2d, each 4.8-chain is shown connected to 6 neighboring chains via L1 ligands to form a 3D structure.

Crystal Structure of [Zn₃(HPO₄)₃(H₂PO₄)(C₂₂H₂₂N₈)_{0.5}–(C₂₂H₂₄N₈)_{0.5}] (3). The reaction of zinc phosphate with L3 yields the two crystalline phases **3** and **7**. These are separated manually by differences in crystal morphology. Compound **7** gives crystals of insufficient quality for a determination of the complete structure, which appears to be a 3D hybrid framework, and the refinement is not of a high enough quality for publication. A complete structure of the compound designated as **3** was determined. The asymmetric unit of **3** contains three crystallographically distinct Zn atoms and four P atoms, as shown in Figure 3a. Each zinc atom is tetrahedrally coordinated by three phosphate oxygen atoms and one imidazole nitrogen from L1: (Zn1–O)_{av} = 1.946 Å, (O–Zn1–O)_{av} = 109.4°, (O–Zn1–N)_{av} = 108.8°; (Zn2–O)_{av} = 1.935 Å, (O–Zn2–O)_{av} = 109.9°, (O–Zn2–N)_{av} = 108.7°; (Zn3–O)_{av} = 1.941 Å, (O–Zn3–O)_{av} = 111.7°, (O–Zn3–N)_{av} = 107.0°. Of the four phosphate groups, P1 coordinates to two zinc atoms, P2 and P3 coordinate to three zinc atoms, and P4 coordinates to one zinc atom. The P–O distances [(P1–O1) = 1.590(3), (P2–O5) = 1.564(3), (P3–O10) = 1.563(3), (P4–O13) = 1.576(3), and (P4–O16) =

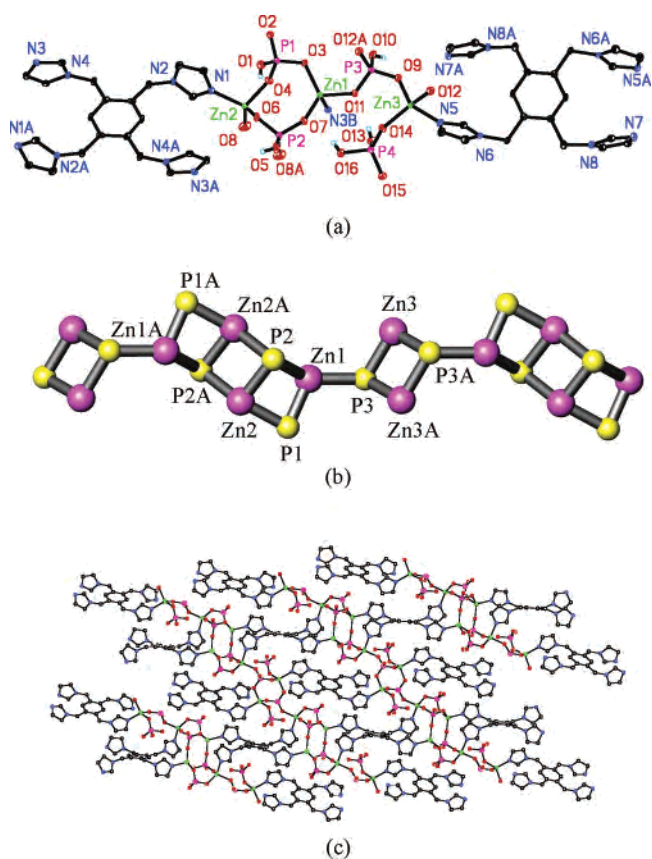


Figure 3. (a) Crystal structure of compound **3** with atom labeling scheme. Thermal ellipsoids are drawn at 50% probability. (b) Schematic drawing of the 1D chain in **3**. (c) 2D structure of compound **3**.

1.590(3) Å] indicate that the terminal oxygens (O1, O5, O10, O13, and O16) are –OH groups.²¹

As shown in Figure 3b, the inorganic structure of **3** consists of a one-dimensional chain constructed from alternating 4-rings and triple fused 4-rings that are connected through one vertex. The 4-rings are composed of vertex-sharing Zn3 and P3 tetrahedra, and the tetrahedral coordination environment of Zn3 is completed by two P3 bridging groups, an L2 ligand (N5), and a pendant P4 group. The triple fused 4-ring is composed of three edge-sharing 4-rings of ZnO₃N (Zn1 and Zn2) and HPO₄ (P1 and P2) tetrahedra. The 4-ring is a well-known secondary building unit, and the triple fused 4-ring has recently been suggested as a tertiary building unit.¹⁰ The chain structure composed of the strictly alternating 4-ring and triple fused 4-ring is new and may be described as arising from the self-assembly of triple 4-rings and 4-rings. Alternatively, it may be considered to be a frustrated ladder structure in which the pendant phosphate group prevents the formation of the ladder motif.

Compound **3** contains two types of L2 ligands: one coordinates to four zinc atoms as a tetradentate bridging ligand, and the other coordinates to two zinc atoms as a bidentate bridging ligand, as seen in the partial packing diagram in Figure 3c. The fragment, [Zn₃(HPO₄)₃(H₂PO₄)₂], has a net framework charge of –2 which is balanced by the diprotonation of the two unligated imidazole groups of the bidentate bridging L2 ligand. To confirm the assignment, the hydrogen atoms attached to the free arms (N7 and N7A)

(21) Brown, I. D.; Aldermatt, D. *Acta Crystallogr.* **1984**, *B41*, 244.

(22) (a) Gordon, L. E.; Harrison, W. T. A. *Acta Crystallogr.* **2004**, *C60*, m637. (b) Harrison, W. T. A. *Int. J. Inorg. Mater.* **2001**, *3*, 179. (c) Ayi, A. A.; Choudhury, A.; Natarajan, S.; Rao, C. N. R. *J. Mater. Chem.* **2000**, *10*, 2606. (d) Zhang, D.; Shi, Z.; Dong, W.; Fu, W.; Wang, L.; Li, G.; Feng, S. *J. Solid State Chem.* **2004**, *177*, 343.

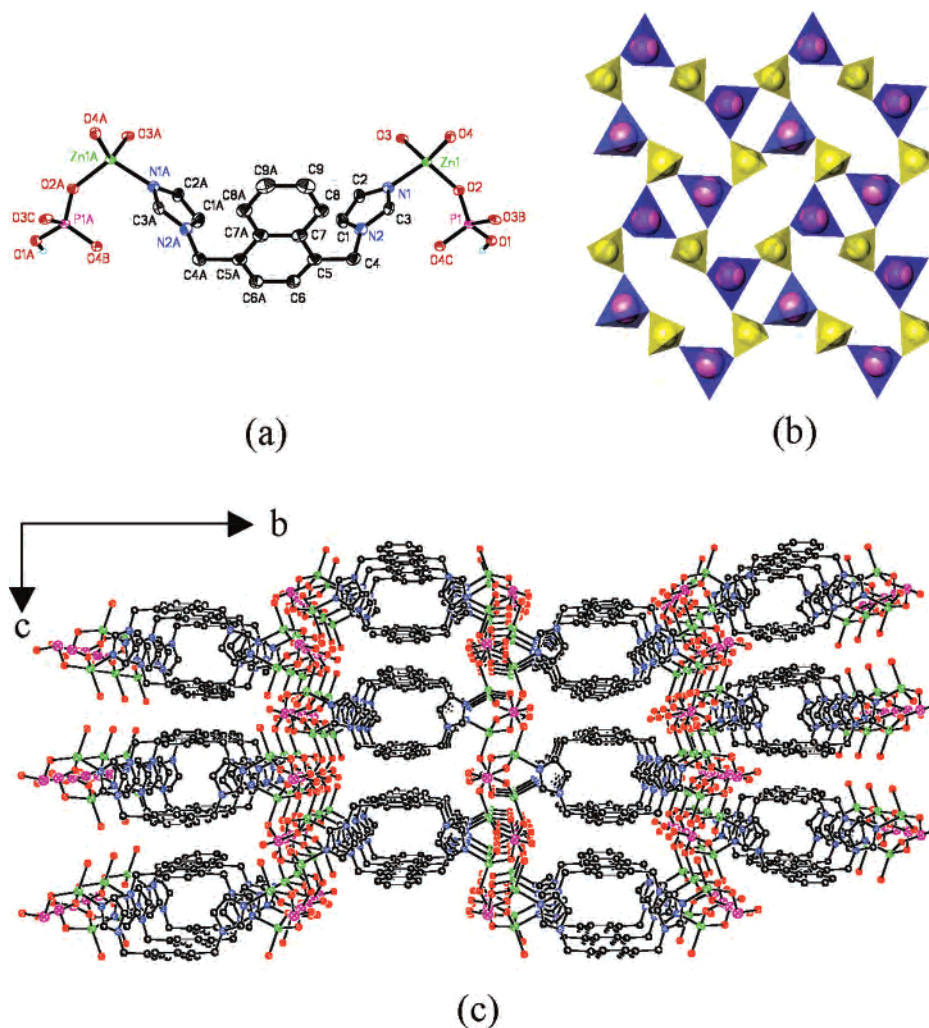


Figure 4. (a) Crystal structure of compound **4** with atom labeling scheme. Thermal ellipsoids are drawn at 50% probability. (b) Polyhedral representation of the 2D sheet in **4** (Zn: blue, P: yellow). (c) Packing diagram of compound **4**.

are located in the residual e^- density map and refined independently. Thus, one L2 ligand in **3** plays the dual role of template and ligand in the stabilization of the structure.

The chains in **3** are linked together by the L2 ligands to form a two-dimensional (2D) sheet. The tetradentate ligand coordinates to the four zinc atoms of the triple fused 4-ring, and the bidentate ligand coordinates to the two zinc atoms of the 4-ring. The protonated imidazole groups of the bidentate ligand are hydrogen bonded to the adjacent sheets through interaction with the P1 group [(N7 \cdots O2) = 2.646(5) Å, and (N7–H7B–O2) = 177°.] The layer structure of **3** is held together via hydrogen bonding in an *ABAB* pattern to form the 3D structure. A packing diagram for **3** is provided in the Supporting Information.

Crystal Structure of [Zn₂(HPO₄)₂(C₁₈H₁₆N₄)] (4**) and [Zn(HPO₄)(C₁₈H₁₄N₂)] (**5**).** The asymmetric unit of compound **4** contains a crystallographically independent zinc atom, a phosphate group, and half of an L3 ligand, as shown in Figure 4a. Each zinc atom is tetrahedrally coordinated by three oxygens from phosphate groups and a nitrogen from L3 [(Zn1–O)_{av} = 1.938 Å, (O–Zn1–O)_{av} = 112.7°, and (O–Zn1–N)_{av} = 106.1°]. Each phosphate group coordinates to three zinc atoms through P–O–Zn linkages [(P–O–Zn)_{av}

= 129.0°]. The longest P–O distance [(P1–O1) = 1.569(3) Å] indicates that the terminal oxygen (O1) is an –OH group.

As shown in Figure 4b, the inorganic framework in **4** consists of a two-dimensional network constructed from edge-sharing 4-rings and 8-rings, with a 4.8² topology. Two types of 4.8² patterns are commonly observed: one with elongated 8-rings in a herringbone pattern^{6h} and one with 8-rings that more closely approximate octagons.¹⁰ It is evident that the 4.8² pattern of **4** has elongated 8-rings. The L3 ligand adopts a *cis* conformation with two imidazole groups extending to the same side of the naphthalene ring. The dihedral angle between the imidazole and naphthalene is 82.0°. The sheets are connected by L3 ligands to form a 3D structure. Specifically, the sheets are covalently pillared by L3 ligands as shown in Figure 4c. In zinc phosphates/phosphites containing 4.8²-sheets, the layer structure is often pillared by ligands, H-bonds, or Zn–O–P linkages.^{10,22} A striking feature of the interlayer pillars is the stacking of the organic ligands to give rise to a small hydrophobic channel of the dimensions 4.2 Å × 4.8 Å that extends through the entire structure parallel to the sheets. The distance between the parallel ZnPO sheets in **4** is 11.23 Å.

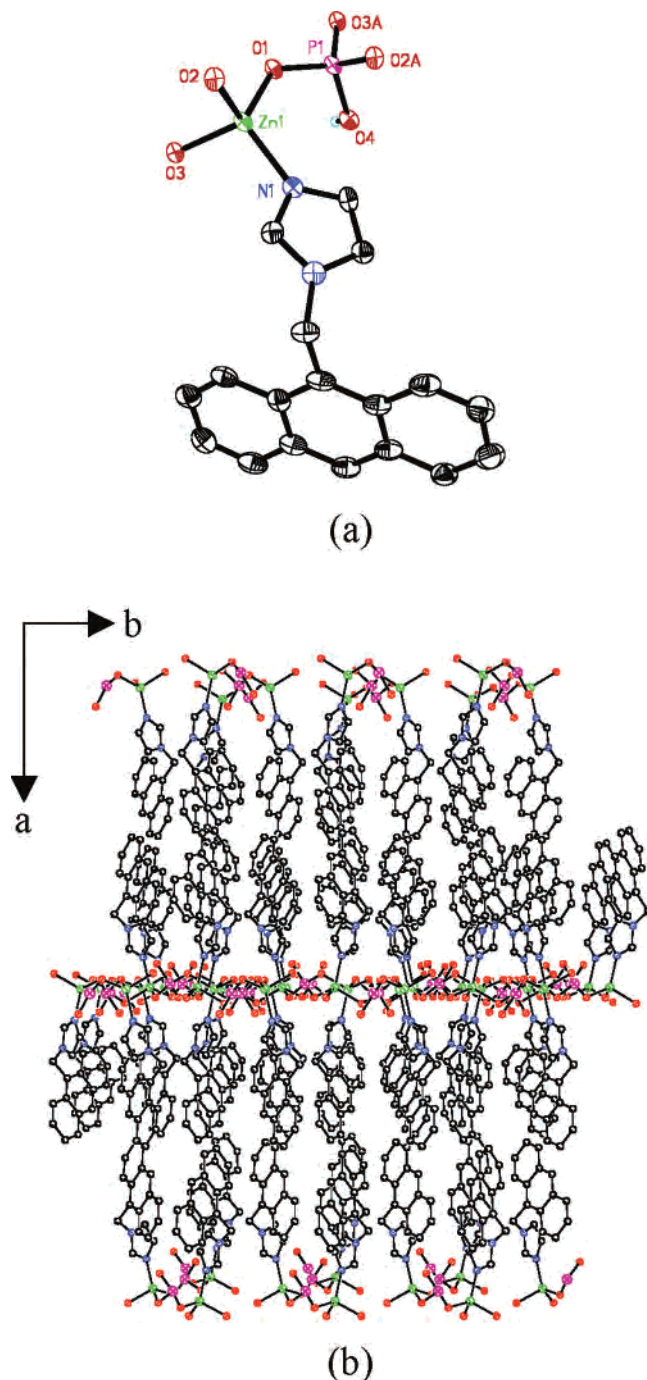


Figure 5. (a) Asymmetric unit of the structure of compound **5** showing the atom labeling scheme. Thermal ellipsoids are drawn at 50% probability. (b) Packing diagram of compound **5**.

The asymmetric unit in **5** contains one crystallographically independent zinc atom, a phosphate group, and an L4 ligand, as illustrated in Figure 5a. The zinc phosphate portion of the structure is again a 4.8²-sheet with a herringbone pattern of 8-rings similar to that observed in compound **4**. In **5**, the sheet is decorated on both sides by the monodentate L4 ligand. Thus, the sheets are neutral and held together only by van der Waals forces to form a 3D structure. A packing diagram is shown in Figure 5b. The nearest approach between anthracene hydrogen atoms from adjacent sheets is 2.65 Å, but there is no π overlap. The shortest H–X contact between anthracene rings associated with a single sheet is 3.06 Å (X

refers to the centroid of the benzene ring) with a C–H–X angle of 130.4°. This indicates weak interactions within each sheet. The packing of anthracene groups on one side of a zinc phosphate sheet mimics the herringbone pattern of 8-rings in the 4.8²-net. That is, there is one anthracene ring per 8-ring on each side of the zinc phosphate plane and each fills the space above an 8-ring with the long axis of anthracene projected onto the long axis of the 8-ring. The zinc atoms within a sheet are coplanar, and the distance between the layers is 19.72 Å.

Structure of Compound [Zn₂(HPO₄)₂(C₁₂H₁₀N₄)] (6**).** Compound **6** is formed from zinc phosphate and the rigid bidentate ligand L5. The asymmetric unit of compound **6** contains one crystallographically independent zinc atom, a phosphate group, and half of an L5 ligand, as shown in Figure 6a. Each zinc atom is tetrahedrally coordinated by three phosphate oxygen atoms and a nitrogen from L5 [(Zn1–O)_{av} = 1.942 Å, (O–Zn1–O)_{av} = 111.9°, and (O–Zn1–N)_{av} = 106.8°]. Each phosphate group coordinates to three zinc atoms through P–O–Zn linkages [(P–O–Zn)_{av} = 121.8°].

As shown in Figure 6b, the inorganic layer in **6** is composed solely of 6-rings to give a 6³ topology. The 6-ring in zinc phosphates is known,²³ specifically in the sodalite structure; however, the planar 6-ring pattern, as in **6**, has not been observed previously for zinc phosphates. Recently, Harrison reported a three-dimensional zinc phosphite structure, (C₆N₂H₈)_{0.5}·ZnHPO₃, in which an inorganic sheet with the 6³ topology is pillared by 1,4-diamino benzene.^{6b} In **6**, the parallel zinc phosphate sheets are linked by L5 ligands. The ligands on opposite sides of the sheets lean significantly from the perpendicular; the major axis of the ligands has an angle of about 50° with respect to the sheet. Thus, the pillars lean significantly to compress the interlayer spacing to 8.3 Å in the 3D structure. The packing of the sheets and the L5 pillars is shown in Figure 6c.

Discussion

Of the five ligands used to prepare six new zinc phosphate phases in this study, the two with the greatest flexibility, L1 and L2, lead to mixtures of products. Compounds **1** and **2** form with L1; compound **3** and the structurally uncharacterized phase **7** form with L2. The observation of mixed products with these ligands is attributed to the flexibility and multifunctionality of L1 and L2.

Compounds **1** and **3** contain both HPO₄²⁻ and H₂PO₄⁻, while compounds **2**, **4**, **5**, and **6** contain only HPO₄²⁻. Further, the stoichiometry of **1** and **3** requires extraframework cations to balance the net anionic charge of the frameworks. Diprotonated L1 serves the role of extraframework cation in **1**, and in **3**, two imidazole groups of the tetradentate ligand L2 are protonated. Dihydrogen phosphate and substituted imidazoles have similar pK_a's. Thus, these systems that

(23) (a) Kongshaug, K. O.; Fjellvag, H.; Lillerud, K. P. *Solid State Sci.* **2000**, *2*, 569. (b) Rodgers, J. A.; Harrison, W. T. A. *J. Mater. Chem.*, **2000**, *10*, 2853. (c) Feng, P.; Bu, X.; Stucky, G. D. *Angew. Chem., Int. Ed. Engl.* **1995**, *34*, 1745. (d) Jensen, T. R.; Norby, P.; Stein, P. C.; Bell, A. M. T. *J. Solid State Chem.* **1995**, *117*, 39.

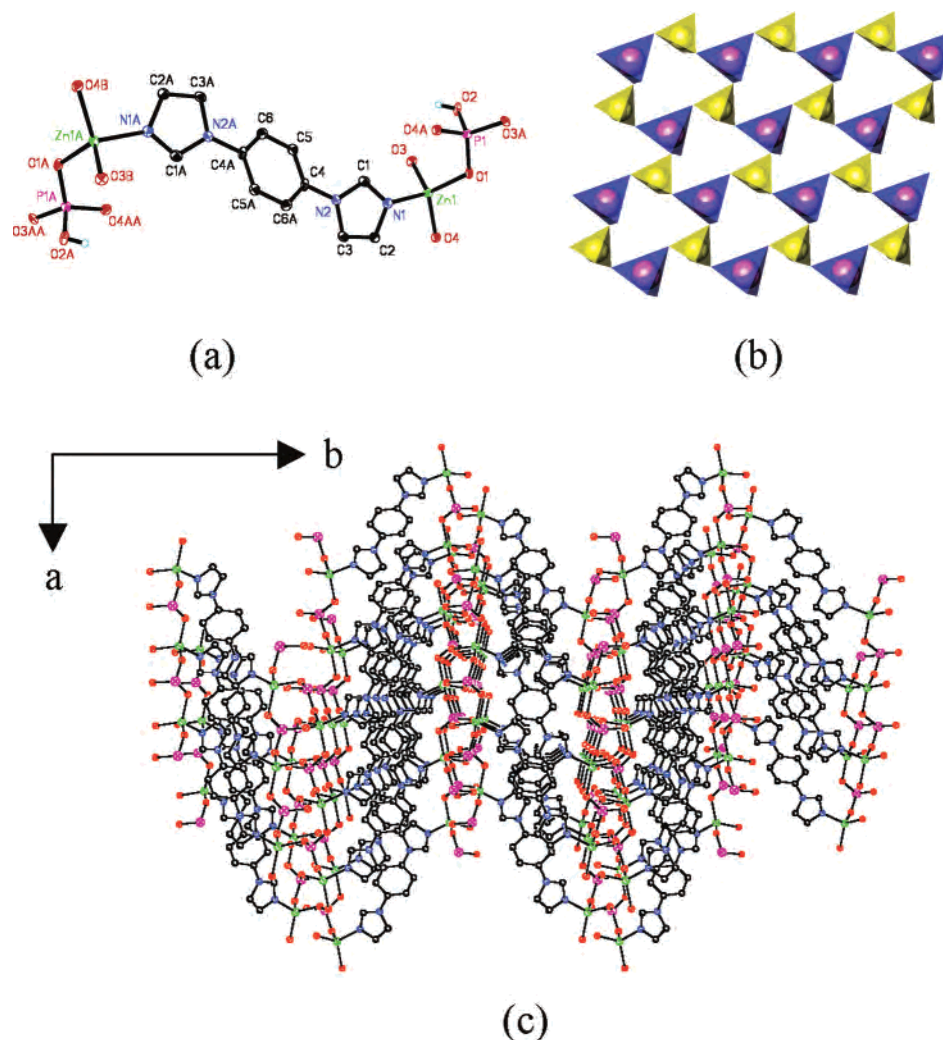


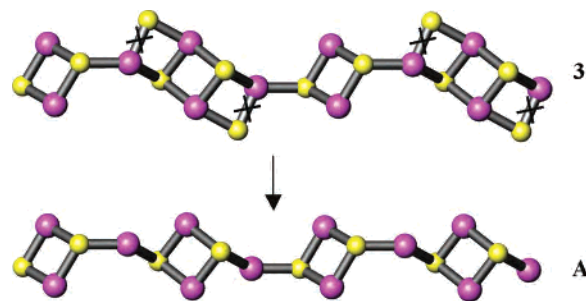
Figure 6. (a) Crystal structure of compound **6** with atom labeling scheme. Thermal ellipsoids are drawn at 50% probability. (b) Polyhedral representation of the 2D sheet in **6** (Zn: blue. P: yellow). (c) Packing diagram of compound **6**.

contain both phosphoric acid and imidazole have flexibility in the location of protons required for charge balance. Though the exact mechanism in the aufbau process is far from being understood, it is certain that the ligand and solution pH play important roles.

In the ligand modified zinc phosphate structures reported here and in the literature, there appears to be a competition between nitrogen donor atoms and phosphate oxygen for zinc coordination sites. Thus, one can envision alternative structures for many ligand/metal combinations. For example an alternative for **3** could have been formed by the additional coordination of the zinc atom in the terminal rings of the triple 4-ring with concomitant deprotonation of the L2. This could lead to structure A as illustrated in Scheme 2. Such a structure remains hypothetical.

The incorporation of multifunctional ligands into zinc phosphate frameworks is a powerful route for the synthesis of inorganic/organic hybrid materials. Imidazole and benzimidazole groups are effective competitors with phosphate ions for zinc coordination sites. This leads to the cleavage of zinc phosphate phases into fragments that include rings, chains, and sheets. The manner in which the inorganic fragments can be put together to form hybrid materials is

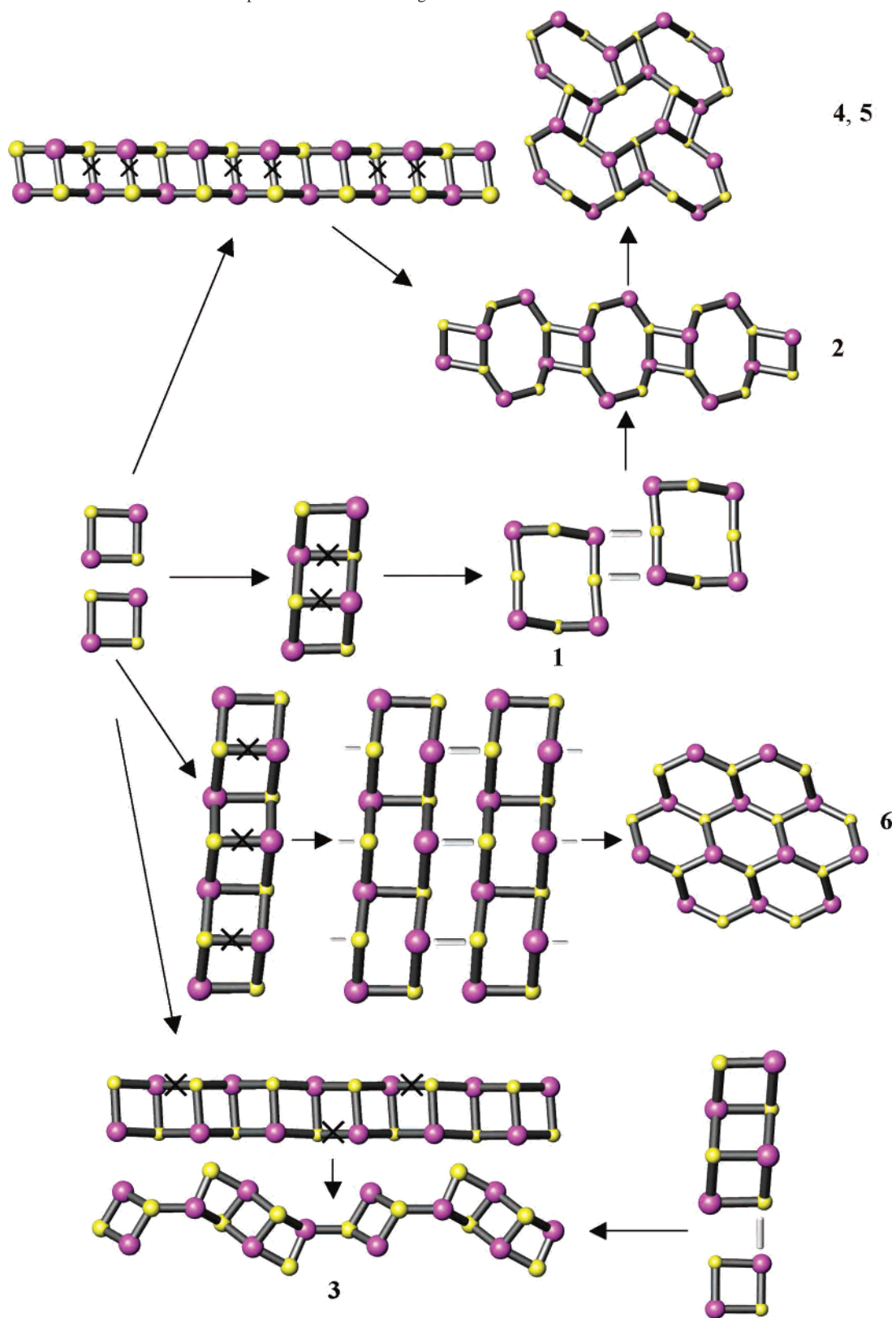
Scheme 2. Possible Transformation of the Chain Observed in **3** To Give a Hypothetical Chain of 4-Rings Linked by Zinc Atoms (Zn: Pink, P: Yellow)^a



^a Pendant phosphate groups on 4-rings are omitted for clarity.

dictated by the ligand and the coordination requirements of the fragments. From the structures described above, it appears that the inorganic pieces in **1**, **2**, **4**, and **5** are closely related as illustrated in Scheme 3. Starting from the commonly observed 4-ring, two 4-rings may link together to generate a triple fused 4-ring and triple 4-rings may condense further to give ladders or stair steps. Alternatively, the triple 4-ring may open up to generate single 8-rings such as those observed in **1**. The linking of 8-rings along one direction

Scheme 3. Scheme for the Formation of Compounds 1–6 from 4-Rings^a



^a The new connections are represented by short bars (Zn: pink, P: yellow).

generates the 4.8-chain as observed in 2. When 8-rings are connected in two directions, then, 4.8²-sheets are obtained as observed in 4 and 5. The ladder structure can also be considered as a possible intermediate in the formation of the 4.8-chain. For example, if two of every four rungs of a 4-ring

ladder are cleaved, a 4.8-chain results. Similarly, the 6³-sheet can be obtained via the cleavage and connection pattern shown in Scheme 3. The ladder structure may also be cleaved to generate the alternating triple 4-ring/4-ring pattern of 3. Alternatively, the inorganic motif in 3 can be constructed

by the combination of two building blocks, the 4-ring and the triple fused 4-ring.

Conclusion

In this paper, six tailored inorganic zinc phosphate motifs are observed when the ligands L1–L5 modify the zinc ions. At the present time, the size, Zn/P ratio, and the framework of the zinc phosphate phases cannot be controlled as desired. However, potentially porous materials can be expected while the Zn–P phase is linked by rigid ligands. We are currently investigating the use of rigid ligands in the construction of such porous materials.

Acknowledgment. We thank R. J. Reynolds for support of this work through a McNair postdoctoral fellowship to J.F. We thank the NSF (Grant CHE-0131128) for funding the purchase of the Oxford Diffraction Xcalibur2 single crystal diffractometer. We thank Ms. Liangming Hu for the TGA. We thank Mark Elvington for the emission spectra.

Supporting Information Available: Figure S1, showing the packing diagram of **3**, and X-ray crystallographic files in CIF format. This material is available free of charge via the Internet at <http://pubs.acs.org>.

IC050314T